

Comprehensive genomic profiling and expression dynamics of the HSP gene family in *Cipangopaludina chinensis* under temperature stress

Xiaoxiao Wu^{1,2#}, Wenqi Yang^{1,2#}, Rui Chen¹, Sisi Chen¹, Quanqing Sun¹, Qiuting Ji¹, Yiqi Sun¹, Siyao Zhao¹, Zhongcheng Wei¹, Fujun Xuan¹, Wu Jin³, Daizhen Zhang^{1*}, Boping Tang^{1*} and Gang Wang^{1*}

¹ Jiangsu Provincial Key Laboratory of Coastal Wetland Bioresources and Environmental Protection, Jiangsu Synthetic Innovation Center for Coastal Bio-agriculture, Yancheng Teachers University, Yancheng 224007, China

² College of Fisheries and Life Science, Shanghai Ocean University, Shanghai 201306, China

³ Key Laboratory of Integrated Rice-Fish Farming Ecology, Ministry of Agriculture and Rural Affairs, Freshwater Fisheries Research Center, Chinese Academy of Fishery, Wuxi 214081, China

Authors contributed equally: Xiaoxiao Wu, Wenqi Yang

* Corresponding authors, E-mail: daizhen79wenxin@163.com; boptang@163.com; baiwang0708@163.com

Abstract

Heat shock proteins (HSPs) play a crucial role in the survival of organisms by facilitating their response to various stress conditions. *Cipangopaludina chinensis* is an important aquaculture species in China that is highly resistant to temperature changes. To better understand the adaptation mechanisms of *C. chinensis* to temperature fluctuations, we identified and analyzed the HSPs in *C. chinensis* (CchHSPs). The 36 identified CchHSPs are distributed on nine chromosomes, and the proteins they encode predominantly exhibit alpha-helix structures. In phylogenetic analyses, each HSP subfamily formed a monophyletic clade. Different CchHSPs showed specific high expression in different tissues. In addition, CchHSP70-09, CchHSP70-12, and CchHSP90-02 were identified as hub genes in the protein-protein interaction network, and the significant elevation of the expression of these genes in foot muscle under heat stress further validated their importance for the adaptation of *C. chinensis* to environmental stress. This study advances our understanding of the mechanisms underlying the adaptability and stress resistance conferred by the HSP gene family in *C. chinensis*. These insights will facilitate future efforts aimed at designing molecular markers and conducting molecular breeding programs for this economically valuable species.

Citation: Wu X, Yang W, Chen R, Chen S, Sun Q, et al. 2025. Comprehensive genomic profiling and expression dynamics of the HSP gene family in *Cipangopaludina chinensis* under temperature stress. *Genomics Communications* 2: e009 <https://doi.org/10.48130/gcomm-0025-0009>

Introduction

Heat shock proteins (HSPs) are molecular chaperones important for responding to various biotic and abiotic stressors, ubiquitously present from higher organisms to bacteria^[1]. Primarily, HSPs assist in proper protein folding, assembly, and refolding, maintaining protein conformation stability, and participating in numerous biological processes such as macromolecular assembly, polypeptide degradation, and transcription regulation^[2–4]. They enhance cellular stress resistance and are closely associated with temperature adaptability^[5]. Under stressful conditions like extreme temperatures and drought, HSPs modulate the organism's stress response, minimize cellular damage, promote repair, and facilitate rapid adaptation to the external environment^[6].

Since the discovery of HSPs in 1962^[7], the involvement of these proteins in processes including stress resistance, apoptosis, and inflammatory responses in living organisms has been the subject of extensive research^[8–10]. The structure and function of HSPs are highly conserved, and the family of HSPs can be subdivided on the basis of molecular weight and structure, into the following subfamilies: HSP100, HSP90, HSP70, HSP60, HSP40, and the small HSPs (sHSP)^[11,12]. Some studies have already focused on HSPs in mollusks^[13–15]. In *Octopus vulgaris*, HSP90 is associated with somatic cell growth and shows higher transcription levels with increased growth rates^[16]. HSP90 plays a pivotal role in the transduction of multiple hormone and growth factor receptors and is essential for cell viability under certain growth conditions^[17,18]. Chen et al. found that HSP70 interfered with apoptosis caused by high expression of cytochrome c under salt stress in *Crassostrea gigas*^[19]. Previous

studies have shown that HSP70 is involved in endoplasmic reticulum stress-induced apoptosis and affects the expression of apoptosis regulatory proteins^[20]. In addition, another study has evidenced a notable elevation in HSP40 expression levels in *Venerupis philippinarum* in response to vibrio challenge or heavy metal stress^[21]. This finding substantiates the pivotal role of HSP40 in the immune response of this species. In the study of the HSP gene family in *Pomacea canaliculata*, each family formed monophyly on the phylogenetic tree, and more genes showed stronger transcription level under heat stress than under cold stress^[13]. Cold stress may induce the expression of HSP70, which is helpful in maintaining the normal physiological function of cells at low temperatures^[22]. In one study, the changes of gene expression of *Ericerus pela* in China under low temperatures were analyzed by WGCNA, among which HSPs were identified as hub genes, and HSPs may play an important role in cold adaptability^[23]. These studies show that organisms can effectively cope with temperature stress and enhance their environment viability through the regulation of HSP gene expression^[24].

The Chinese mysterysnail (*Cipangopaludina chinensis*) belongs to the phylum Mollusca, class Gastropoda, and the family Viviparidae. This species is one of the few commercially significant edible freshwater snails in the Chinese market, possessing substantial economic value. In recent years, an increasing number of farmers have elected to engage in *C. chinensis* breeding in captivity, to satisfy the substantial demand for these snails in the Chinese market. *C. chinensis* exhibits a wide adaptation, occurring in a range of aquatic habitats, including paddy fields, lakes, and rivers^[25]. This species of snail allows its young to develop within the maternal body before

oviposition^[26]. This ovoviviparous reproduction plays a role in its reproductive strategy in harsh environments^[27]. In addition, *C. chinensis* demonstrates remarkable resilience to a range of environmental stressors, including drought, heat, cold, and water pollution^[28]. This adaptability contributes to its extensive distribution in freshwater ecosystems across China.

The identification of gene families facilitates an in-depth comprehension of the biological characteristics and evolutionary history of species^[26,29]. At present, there is a paucity of research on gene families of viviparids. To enhance comprehension of the molecular mechanisms underpinning the extensive adaptation of viviparids, including *C. chinensis*, we have conducted a comprehensive genome-wide identification and characterization of the HSP gene family of *C. chinensis*. This study provides supplementary data to the existing body of research on HSPs in this species, offering a foundation for future investigations into functional gene studies, molecular breeding, and genetic engineering in this species.

Materials and methods

Identification of the HSP gene family in Chinese mysterysnail

The HSP gene family of *C. chinensis* (CchHSPs) was identified using genomic data from our laboratory that had been uploaded to the China National Center for Bioinformation (Project No. PRJCA032441).

According to the published HSP gene family of the *P. canaliculata*^[13] as reference sequences, the protein sequence was compared with those of *C. chinensis* using Blastp software^[30], with the parameter set to E-value $\leq 1e^{-9}$ to identify candidate protein sequences. The candidate HSP gene family was screened and confirmed using HMMER software^[31] in combination with the specific domains of the HSP gene family (HSP90: PF00183; HSP70: PF00012; HSP60: PF00118; HSP40: PF00226; HSP20: PF00011; HSP10: PF00166).

The chromosomal location of CchHSPs was extracted from the genome annotation file of *C. chinensis* using TBtools v2.119 software^[32]. The tandemly arrayed gene file obtained from intraspecific collinearity analysis was also verified using TBtools software.

Characterization prediction of CchHSPs

The candidate protein sequences were analyzed for conserved domains using the online SMART tool (<http://smart.embl-heidelberg.de>). Subsequently, the protein sequences of the identified HSP gene family were evaluated using the ProtParam tool on the ExPASy website (web.expasy.org/protparam), which calculated their amino acid length (aa), theoretical isoelectric point (pI), and molecular weight (MW). The subcellular localization of these proteins was predicted using the CELLO online server (<http://cello.life.nctu.edu.tw>).

The intron, exon, and non-coding region structures were visualized using the GSDS2.0 online tool (<http://gsds.gao-lab.org>). The conserved motifs of the CchHSPs were predicted and analyzed using the MEME suite (<http://meme-suite.org/tools/meme>). The maximum limit number of detected motifs was set to 20, with functional domain lengths ranging from 30 to 100 amino acid residues. The minimum number of occurrences for the functional domain was set to 10, while other parameters remained at default settings^[33]. The domain structure of CchHSPs was predicted using NCBI's BatchCD-Search tool (www.ncbi.nlm.nih.gov/Structure/bwrpsb/bwrpsb.cgi), and all domain sequences were extracted based on the predicted positions. The secondary structure of CchHSPs was predicted using the GOR4 online tool (https://npsa-prabi.ibcp.fr/cgi-bin/npsa_automat.pl?page=npsa_gor4.html), and the 3D protein

structures were modeled using the SWISS-MODEL interactive website (<https://swissmodel.expasy.org/interactive>).

To analyze the protein interaction network of CchHSPs, the protein sequences were uploaded to the STRING online database (<https://cn.string-db.org/>), with *P. canaliculata* serving as the model. The maximum number of interactions displayed was set to 10 for the first layer, and 20 for the second layer.

Phylogenetic analysis of the HSP gene family in gastropods

To further investigate the relationship of HSP gene families among *C. chinensis* and its relatives, we also used the uploaded genomic data in the National Center for Biotechnology Information (NCBI) database to identify the HSP gene families of *Pomacea maculata* (GCA_004794325.1), *Biomphalaria glabrata* (GCA_000457365.2), *Achatina fulica* (PRJNA511624), *Lautoconus ventricosus* (GCA_018398815.1), and *Patella pellucida* (GCA_917208275.1). In addition, the *B. aeruginosa* genome obtained from our laboratory was similarly identified for the HSP gene family. Afterward, the protein sequences of the HSP gene family of these seven snails were compared using the default parameters of the MEGA11 software^[34]. A phylogenetic tree was constructed using the maximum likelihood (ML) method, with the Jones-Taylor-Thornton (JTT) model employed for ML algorithm analysis. Additionally, a separate ML phylogenetic tree was constructed specifically for *C. chinensis*. The resulting phylogenetic trees were enhanced using the tvBOT website^[35].

Expression levels of CchHSPs in various tissues

Total RNA was individually extracted from the antenna, labial palp, foot muscle, testis, ovarian endometrium, kidney, gill, and mantle tissues of *C. chinensis* using an RNA extraction kit (TaKaRa Bio, Dalian, China). After verifying RNA integrity through agarose gel electrophoresis, total RNA concentration was measured with a micro-UV spectrophotometer (MaestroGen, Taiwan, China). Samples with an OD260/OD280 ratio between 1.8 and 2.0 were selected and sent for sequencing (Fraser Biotech, Wuhan, China). Transcriptome sequencing was performed using a HiSeq4000 sequencer (Illumina, CA, USA) with a read length of 150 PE. The transcriptome data were filtered, and quality controlled using Trimmomatic v0.38 software^[36]. RNA-seq data are aligned with the reference genome of *C. chinensis* from this paper using the default parameters of Hisat2 v2.1.0 software^[37]. The data were then aligned with the reference genome, and gene expression levels for each tissue were calculated using featurecounts v2.0.1^[38]. The expression levels of each member of the CchHSPs gene family in different tissues were integrated into a matrix. Data normalization and a tissue expression heatmap of the CchHSPs gene family were generated using the heatmap package in R Studio.

Expression levels of CchHSPs under temperature stress

Ninety healthy, uniformly sized female *C. chinensis* (26.42 ± 4.75 g) were selected from Yancheng, China, and placed uniformly and randomly into nine 10 L buckets in the laboratory for three days of acclimatization. Afterward, the water temperature of three buckets was set at 0 °C to subject the snails to cold stress, three buckets were set at 30 °C to subject the snails to heat stress, and the other three buckets were kept at room temperature (24 °C) to serve as a control group. After three days, three snails were randomly sampled from each bucket. Kidney, foot muscle, and gill tissues obtained from each snail were used for subsequent total RNA extraction.

Total RNA was also extracted using an RNA extraction kit (TaKaRa Bio, Dalian, China). The cDNA was synthesized using HiScriptIIqRT SuperMixII (Vazyme Biotech, Nanjing, China), and the primers for Real-Time Polymerase Chain Reaction (qPCR) of the target genes

were designed using Primer Premier 5.0 software^[39]. The primers used are shown in [Supplementary Table S1](#). ChamQ SYBR Color qPCR Master Mix (Vazyme Biotech, Nanjing, China) and QuantStudio3 (Thermo Fisher Scientific, USA) were used for qPCR experiments. The program was conducted as follows: 2 min at 95 °C, 40 cycles (each cycle was for 15 s at 95 °C, 20 s at 56 °C, and 30 s at 72 °C), 30 s at 95 °C, 1 min at 60 °C, and 10 s at 95 °C. Statistical analysis of qPCR results was performed using GraphPad Prism 10 software. Significance levels between groups were analysed using one-way ANOVA and Tukey's post hoc test.

Results

Identification and chromosomal distribution of CchHSPs

Through whole-genome scanning, a total of 36 CchHSPs were identified in the genome of *C. chinensis*, including six subfamilies: CchHSP10 (1), CchHSP20 (8), CchHSP40 (11), CchHSP60 (1), CchHSP70 (12), and CchHSP90 (3) ([Supplementary Tables S2–S3](#)). In *C. chinensis*, chromosome localization analysis revealed that the 36 CchHSPs were distributed across nine chromosomes. Specifically, CchHSP70s were found on Chr1, Chr2, Chr3, Chr5, Chr6, Chr7, and Chr8; CchHSP10 on Chr1; CchHSP20s appeared on both Chr4 and Chr9, CchHSP40s were present on Chr1, Chr2, Chr3, Chr4, Chr6, Chr7, and Chr8, CchHSP60 was identified on Chr1; while CchHSP90s resided on Chr3 and Chr6. Moreover, we identified four clusters formed by tandemly repeated genes: CchHSP20-01 to CchHSP20-05 on Chr4, CchHSP70-01 and CchHSP70-02 on Chr1, CchHSP70-05 and CchHSP70-06 on Chr2, and CchHSP70-10 and CchHSP70-11 on Chr7 ([Fig. 1](#)). The structure of genes within each cluster exhibited high similarity, and the intergenic distances between genes in each cluster were less than 10 kb ([Supplementary Table S4](#)).

Physicochemical properties of CchHSPs

The CchHSPs vary from 102 to 1,102 aa with the CchHSP70s being the longest and the CchHSP10s the shortest. Generally, an increase in the classification within the HSP gene family correlates with an increase in protein sequence length. The molecular weights (MWs) of CchHSPs range from 11.23 to 124.69 kDa. It is evident from the data that both the protein sequence lengths and molecular weights of CchHSP10s and CchHSP20s are relatively small, while those of CchHSP70s and CchHSP90s are significantly larger. The theoretical isoelectric points (pI) of CchHSPs range from 4.82 to 9.21. Among these, 29 members exhibit

a pI between 4.82 and 6.99 (acidic), while seven members have a pI ranging from 7.61 to 9.21 (alkaline) ([Table 1](#)).

The instability index of CchHSPs varies from 28.52 to 62.88, while the aliphatic index ranges from 46.89 to 105.36. GRAVY analysis indicates that all members, except CchHSP70-03, are hydrophilic proteins characterized by a GRAVY value of less than zero. Predictions regarding subcellular localization reveal that 20 CchHSPs were predominantly located in the cytoplasm, nine in the nucleus, three in the mitochondrion, three in the endoplasmic reticulum, and one in the extracellular space. Specifically, CchHSP10s and CchHSP20s are primarily localized within the cytoplasm; CchHSP40s are mainly found in the nucleus; CchHSP60s reside within mitochondria; whereas both CchHSP70s and CchHSP90s predominantly occur in the cytoplasm. Consequently, it can be inferred that CchHSPs primarily execute their functions within these specific subcellular compartments.

Gene structure and protein characterization of CchHSPs

The results of gene structure prediction are shown in [Fig. 2a](#). To investigate the diversity of protein structures of CchHSPs, we predicted their conserved motifs, which resulted in a total of 20 different motifs being identified ([Supplementary Fig. S1](#)). Among these, CchHSP70s exhibited the highest number of conserved motifs, while CchHSP10s displayed the fewest ([Fig. 2b](#)).

The prediction results for the domain of CchHSPs are illustrated in [Fig. 3](#). Two proteins encoded by CchHSP70 possess domains related to the nucleotide-binding domain (NBD). The HSP40 gene family includes characteristic sequences encode for the DnaJ domain, as well as members of the DnaJ superfamily, RRM_DNAJC17, DUF1977, CbpA, PRPK10767 superfamily, and PTZ00037 superfamily domains. Specifically, CchHSP40-02, CchHSP40-03, CchHSP40-04, CchHSP40-07, CchHSP40-08, CchHSP40-09, and CchHSP40-10 all contain the DnaJ domain, which is more commonly referred to as the J domain. The proteins encoded by CchHSP60 were characterized by a distinct GroEL domain; CchHSP10 had a cpn10 structural domain; CchHSP20 had one or two metazoan_ACD structural domains.

The secondary structure of CchHSPs primarily comprises alpha helices, extended strands, and random coils. Among these, random coil amino acids represent the highest proportion (35.10% to 64.81%), followed by alpha helix amino acids (9.94% to 52.20%), and extended strand amino acids, which account for the lowest proportion (10.87% to 27.45%) ([Table 2](#)). Three-dimensional structure

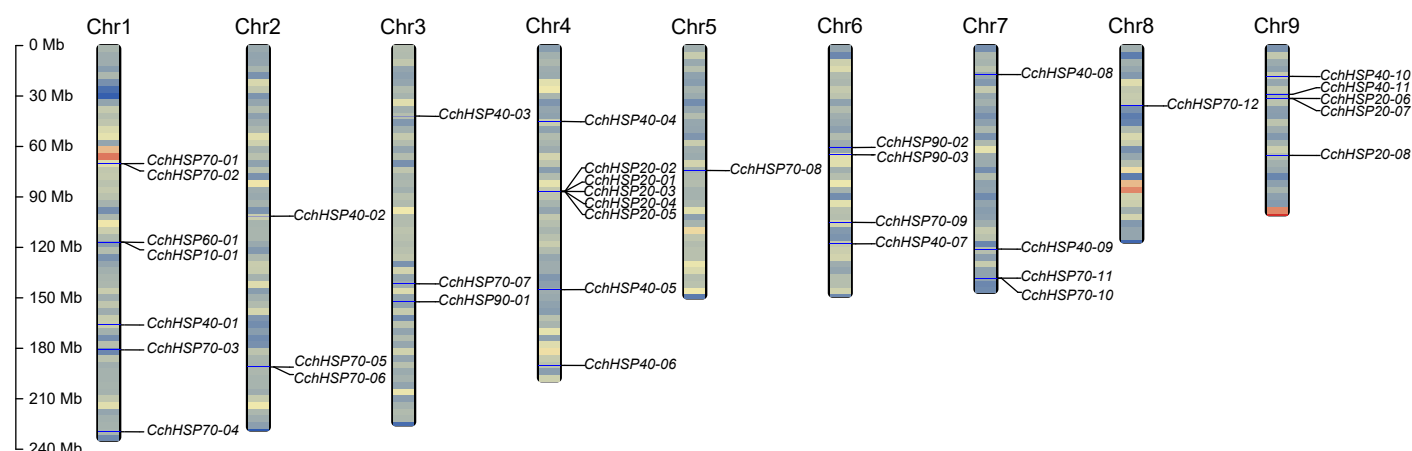


Fig. 1 The chromosomal locations of the identified CchHSPs. The chromosome gene density is expressed by the gradient color of blue-red from low to high.

Table 1. Characteristics summary of HSP genes in *C. chinensis*.

Gene name	Size (aa)	MW (Da)	pI	Instability index	Aliphatic index	Grand average of hydropathicity (GRAVY)	Chromosome no.	Subcellular localization
CchHSP10-01	102	11,232.16	7.95	35.20	95.53	−0.110	Chr1	Cytoplasm
CchHSP20-01	165	18,552.21	5.83	32.45	80.36	−0.445	Chr4	Cytoplasm
CchHSP20-02	260	29,741.03	7.61	44.95	76.85	−0.596	Chr4	Cytoplasm
CchHSP20-03	168	19,473.30	5.83	41.55	72.38	−0.667	Chr4	Cytoplasm
CchHSP20-04	171	19,507.20	5.61	44.42	71.11	−0.629	Chr4	Cytoplasm
CchHSP20-05	167	19,123.81	5.75	43.94	74.67	−0.656	Chr4	Cytoplasm
CchHSP20-06	432	47,398.99	5.94	58.01	62.75	−0.694	Chr9	Nucleus
CchHSP20-07	199	23,147.35	5.37	33.67	64.17	−0.658	Chr9	Cytoplasm
CchHSP20-08	646	73,972.96	6.63	57.22	73.19	−0.784	Chr9	Nucleus
CchHSP40-01	235	25,939.71	6.99	56.68	46.89	−0.697	Chr1	Nucleus
CchHSP40-02	318	35,945.69	8.57	54.98	79.53	−0.823	Chr2	Nucleus
CchHSP40-03	354	38,868.21	8.93	33.87	64.72	−0.631	Chr3	Cytoplasm
CchHSP40-04	317	35,413.31	6.72	36.37	79.62	−0.494	Chr4	Cytoplasm
CchHSP40-05	412	45,624.63	5.89	35.02	66.00	−0.662	Chr4	Nucleus
CchHSP40-06	404	44,884.34	6.40	41.65	74.83	−0.591	Chr4	Nucleus
CchHSP40-07	493	53,964.07	8.95	44.23	70.43	−0.484	Chr6	Mitochondrion
CchHSP40-08	368	42,963.14	8.74	62.88	64.16	−0.986	Chr7	Nucleus
CchHSP40-09	356	40,248.48	5.47	41.35	72.19	−0.619	Chr7	Cytoplasmic
CchHSP40-10	339	40,677.82	9.21	52.62	80.24	−0.696	Chr9	Nucleus
CchHSP40-11	220	24,065.09	5.46	46.26	62.59	−0.540	Chr9	Extracellular space
CchHSP60-01	573	61,096.40	5.69	28.52	98.05	−0.093	Chr1	Mitochondrion
CchHSP70-01	296	32,945.25	4.82	21.95	84.63	−0.626	Chr1	Endoplasmic reticulum
CchHSP70-02	659	72,885.36	5.02	29.26	86.07	−0.494	Chr1	Endoplasmic reticulum
CchHSP70-03	431	47,342.62	5.97	30.02	105.36	0.060	Chr1	Cytoplasm
CchHSP70-04	657	71,936.88	6.63	36.74	82.68	−0.461	Chr1	Mitochondrion
CchHSP70-05	640	70,385.24	5.70	36.86	78.81	−0.499	Chr2	Cytoplasm
CchHSP70-06	640	70,440.41	5.86	37.46	78.81	−0.499	Chr2	Cytoplasm
CchHSP70-07	518	55,978.35	6.18	38.34	89.34	−0.141	Chr3	Cytoplasm
CchHSP70-08	1,102	124,693.00	5.20	37.68	72.29	−0.854	Chr5	Nucleus
CchHSP70-09	855	95,997.61	5.24	44.11	70.95	−0.635	Chr6	Cytoplasm
CchHSP70-10	637	70,158.17	5.77	33.55	79.62	−0.496	Chr7	Cytoplasm
CchHSP70-11	637	70,158.21	5.77	33.39	79.92	−0.491	Chr7	Cytoplasm
CchHSP70-12	649	71,456.75	5.55	37.75	79.52	−0.479	Chr8	Cytoplasm
CchHSP90-01	792	90,870.62	4.91	36.57	81.96	−0.630	Chr3	Endoplasmic reticulum
CchHSP90-02	730	83,874.10	4.93	42.35	79.07	−0.686	Chr6	Cytoplasm
CchHSP90-03	730	83,274.87	6.40	42.29	88.59	−0.409	Chr6	Cytoplasm

MW, molecular weight; pI, isoelectric point.

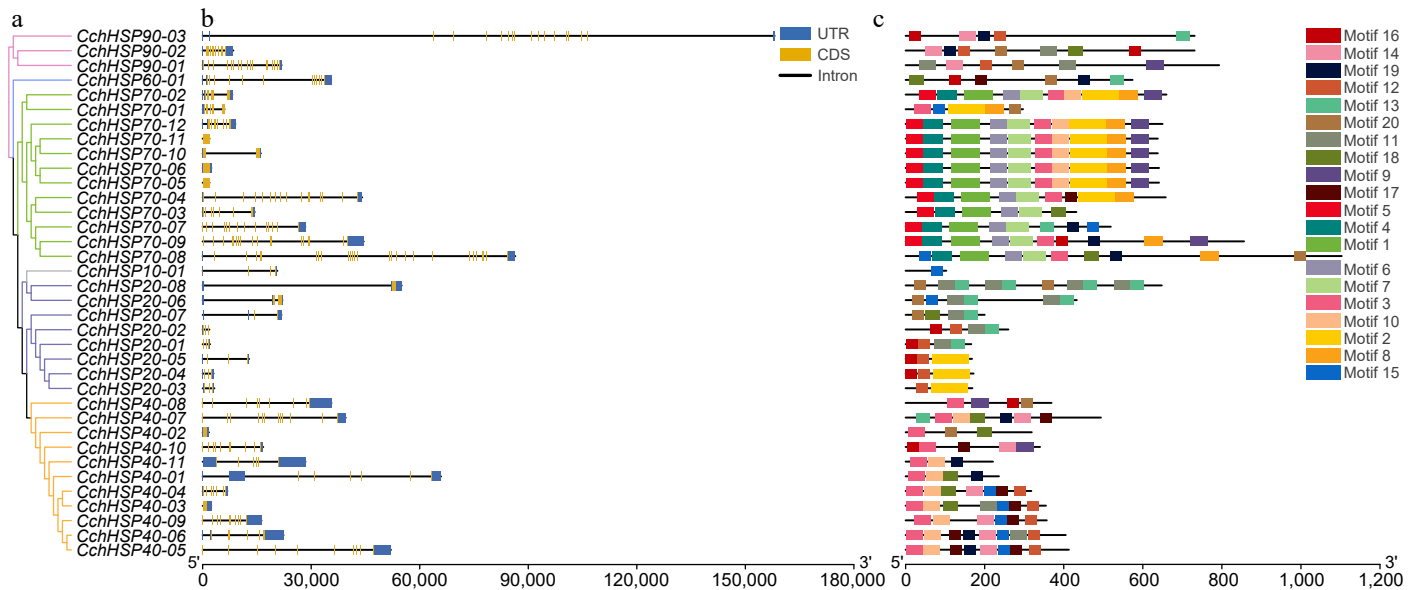


Fig. 2 (a) Phylogenetic relationships of the CchHSPs. (b) Gene structures of the CchHSPs. (c) Conserved motifs of the CchHSPs.

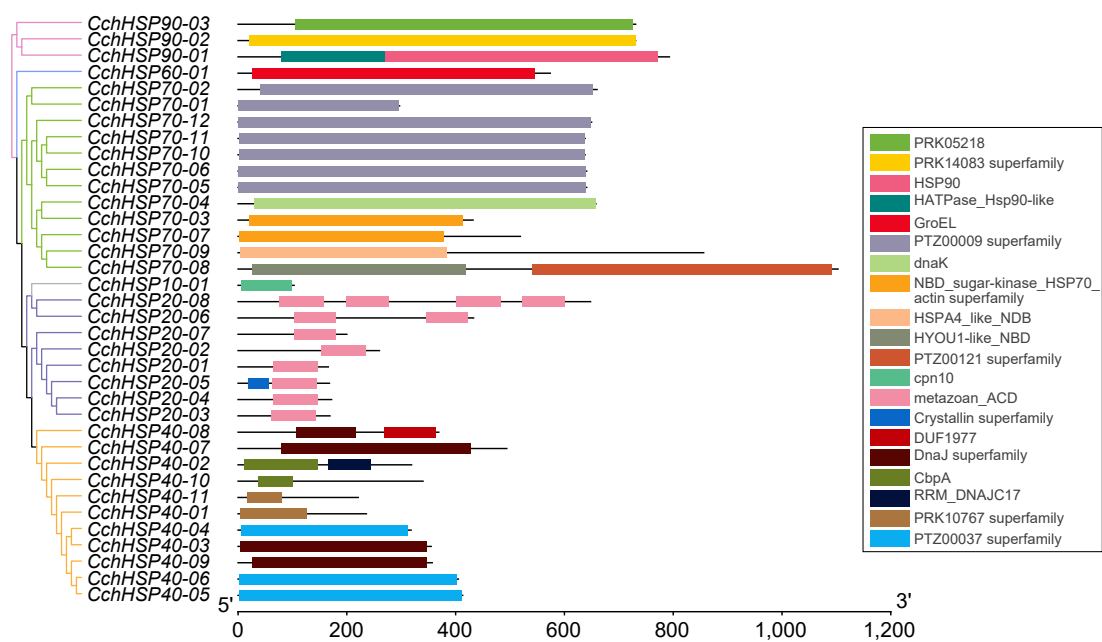


Fig. 3 The protein domain analysis of the CchHSPs.

Table 2. Summary of two-dimensional structures of CchHSPs proteins.

Gene name	Sequence length	Alpha helix (Hh)	Extended strand (Ee)	Random coil (Cc)
CchHSP10-01	102	28/27.45%	28/27.45%	46/45.10%
CchHSP20-01	165	32/19.39%	31/18.79%	102/61.82%
CchHSP20-02	260	45/17.31%	58/22.31%	157/60.38%
CchHSP20-03	168	19/11.31%	41/24.40%	108/64.29%
CchHSP20-04	171	17/9.94%	45/26.32%	109/63.74%
CchHSP20-05	167	39/23.35%	32/19.16%	96/57.49%
CchHSP20-06	432	92/21.30%	60/13.89%	280/64.81%
CchHSP20-07	199	42/21.11%	32/16.08%	125/62.81%
CchHSP20-08	646	204/31.58%	131/20.28%	311/48.14%
CchHSP40-01	235	71/30.21%	41/17.45%	123/52.34%
CchHSP40-02	318	166/52.20%	36/11.32%	116/36.48%
CchHSP40-03	354	85/24.01%	73/20.62%	196/55.37%
CchHSP40-04	317	70/22.08%	72/22.71%	175/55.21%
CchHSP40-05	412	75/18.20%	90/21.84%	247/59.95%
CchHSP40-06	404	108/26.73%	77/19.06%	219/54.21%
CchHSP40-07	493	114/23.12%	96/19.47%	283/57.40%
CchHSP40-08	368	137/37.23%	40/10.87%	191/51.90%
CchHSP40-09	356	111/31.18%	44/12.36%	201/56.46%
CchHSP40-10	339	148/43.66%	72/21.24%	119/35.10%
CchHSP40-11	220	46/20.91%	37/16.82%	137/62.27%
CchHSP60-01	573	298/52.01%	70/12.22%	205/35.78%
CchHSP70-01	296	100/33.78%	58/19.59%	138/46.62%
CchHSP70-02	659	237/35.96%	128/19.42%	294/44.61%
CchHSP70-03	431	190/44.08%	73/16.94%	168/38.98%
CchHSP70-04	657	294/44.75%	101/15.37%	262/39.88%
CchHSP70-05	640	254/39.69%	118/18.44%	268/41.88%
CchHSP70-06	640	254/39.69%	117/18.28%	269/42.03%
CchHSP70-07	518	210/40.54%	84/16.22%	224/43.24%
CchHSP70-08	1102	534/48.46%	133/12.07%	435/39.47%
CchHSP70-09	855	346/40.47%	105/12.28%	404/47.25%
CchHSP70-10	637	257/40.35%	114/17.90%	266/41.76%
CchHSP70-11	637	255/40.03%	114/17.90%	268/42.07%
CchHSP70-12	649	272/41.91%	104/16.02%	273/42.06%
CchHSP90-01	792	395/49.87%	112/14.14%	285/35.98%
CchHSP90-02	730	363/49.73%	91/12.47%	276/37.81%
CchHSP90-03	611	279/45.66%	113/18.49%	219/35.84%

predictions indicate that the genes in sister branches of the same subfamily exhibit similar protein structures (Supplementary Fig. S2).

Phylogenetic analysis of HSPs at both inter- and intra-specific levels

The phylogenetic tree of HSPs in *C. chinensis* was constructed using the maximum likelihood (ML) method (Fig. 4a). The tree is divided into three major branches, with each subfamily gene clustering together separately. Among them, *CchHSP90s*, *CchHSP60*, and *CchHSP70* are closely related, whereas the *CchHSP10s*, *CchHSP20*, and *CchHSP40* families, being relatively large, occupy different branches.

A phylogenetic tree was also constructed utilizing identified HSP protein sequences from *C. chinensis*, *B. aeruginosa*, *P. maculata*, *B. glabrata*, *A. fulica*, *L. ventricosus*, and *P. pellucida* (Fig. 4b). This tree is categorized into four major branches, with genes from each subfamily clustering within their respective branches. Furthermore, gene duplication events were observed within the *HSP70* subfamily (specifically between *CchHSP70-05* and *CchHSP70-06* as well as between *CchHSP70-10* and *CchHSP70-11*). The clustering of HSP subfamily genes across species underscores the high reliability of this phylogenetic analysis.

Protein-protein interaction network of CchHSPs

Using the STRING, an interaction network analysis of *C. chinensis* proteins was conducted with *P. canaliculata* as the reference species to identify potential protein interactions (Supplementary Tables S5–S6). The analysis revealed that 26 CchHSPs were involved in protein interactions (Supplementary Fig. S3). Among these, *CchHSP70-9*, *CchHSP70-12*, and *CchHSP90-2* had the most interactions, making them key nodes. These three nodes all interacted with *NEDD8*, *A0A2T7PA24*, and *A0A2T7NZM9* proteins. There was a strong interaction between CchHSP40 genes and CchHSP70 genes. Additionally, the key node *CchHSP90-02* had a strong interaction with the *Elongin-C* and *NEDD8* proteins.

According to STRING function annotations, the *NEDD8* protein is primarily involved in ubiquitin binding, ubiquitin-like protein ligases, biological processes of cellular macromolecules, various protein metabolism pathways, and the regulation of metabolic pathways. The *A0A2T7PA24* protein can bind to *HSP90*, FK506, and

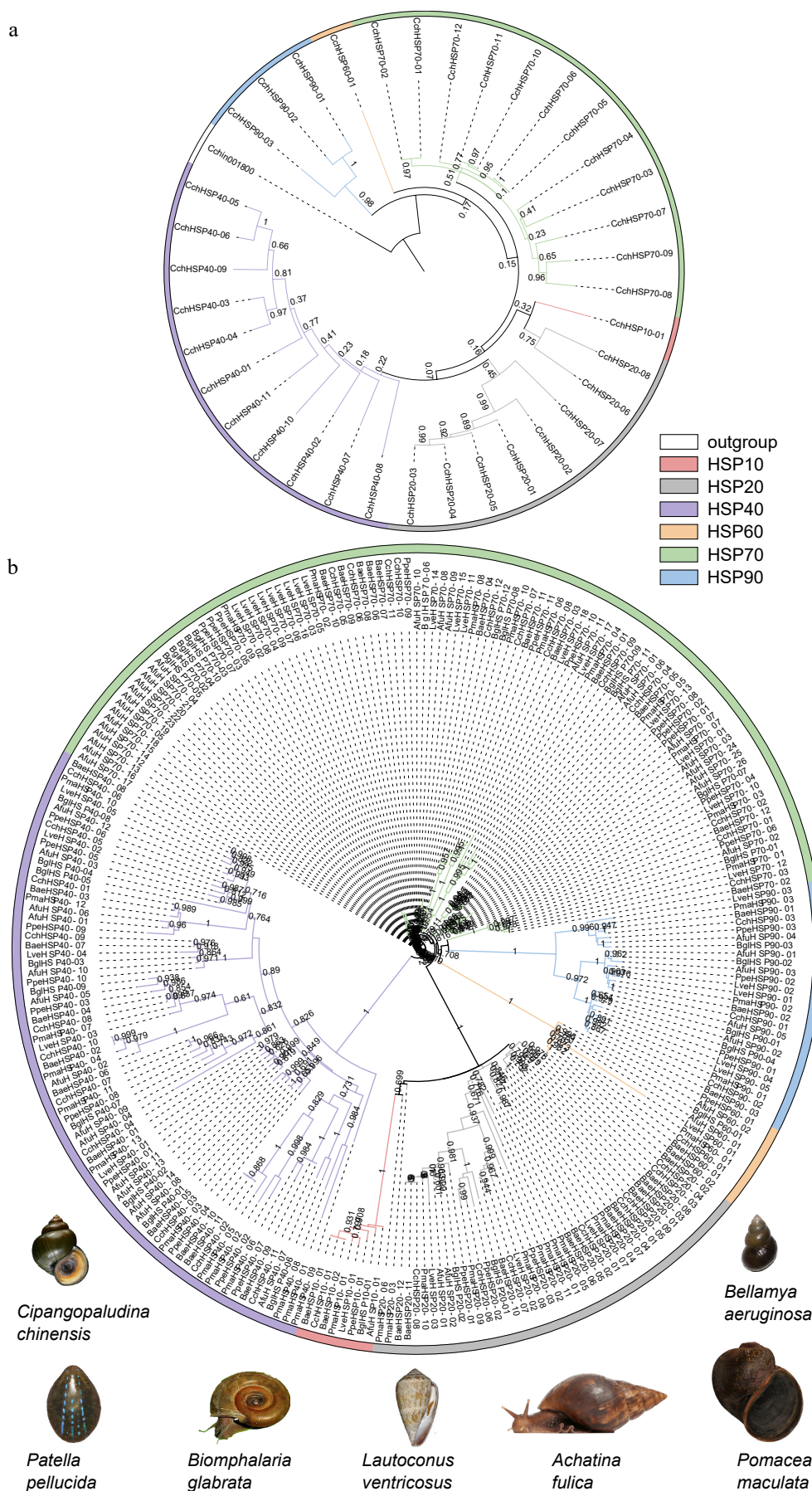


Fig. 4 (a) The phylogenetic tree of the CchHSPs via the maximum likelihood (ML) approach. (b) The phylogenetic analysis for the HSPs in *C. chinensis*, *B. aeruginosa*, *P. maculata*, *B. glabrata*, *A. fulica*, *L. ventricosus*, and *P. pellucida*.

unfolded proteins, participate in the synthesis, degradation, and metabolism of prostaglandins, and regulate the activity of prostaglandin-E synthase. The A0A2T7NZM9 protein can respond to various stimuli such as cytokines and chemicals, like A0A2T7PA24, and has the function of binding to HSPs. It participates in chaperone-mediated protein folding and response to heat and regulates the activity of prostaglandin-E synthase.

Expression profiles of the HSP gene family in different tissues

The expression levels of CchHSPs in different tissues were assessed using RNA-seq data and the results are illustrated in Fig. 5. CchHSP10-01, CchHSP20-02, CchHSP20-04, CchHSP40-03, CchHSP70-12, and CchHSP90-02 exhibited high expression (TPM > 90) in all tissues. The TPM values were further analyzed by one-way ANOVA using R software and Tamhane's T2 method was selected for post hoc comparison. The results showed that CchHSP10-01 expression had the highest expression in the kidney, which was significantly higher than that in the lip and gill ($p < 0.05$). CchHSP20-07 expression was significantly lower in hepatopancreas, ovary, endometrium, kidney, gill, and mantle than in testis ($p < 0.05$). In contrast, the expression of CchHSP40-08 in testis was the lowest and significantly lower than in foot muscle, hepatopancreas, and ovary ($p < 0.05$). CchHSP90-01, CchHSP90-02, and CchHSP90-03 were all highest in testis and all were significantly higher than foot muscle, hepatopancreas, and endometrium ($p < 0.05$).

Effects of heat and cold stress on the expression levels of CchHSPs

C. chinensis has a strong temperature adaptability in natural conditions and can survive in both northern and southern regions of China. In this study, we used 0 and 30 °C as the survival limit temperatures for the snails under stress conditions. In this study, we investigated the expression of seven CchHSPs, namely CchHSP10-01, CchHSP20-02, CchHSP40-03, CchHSP60-01, CchHSP70-09, CchHSP70-12, and CchHSP90-02 in the kidney, gill, and foot muscle of *C. chinensis* using qPCR (Supplementary Tables S7–S9). Our results demonstrated that under high-temperature stress at 30 °C, the expression levels of these genes were significantly elevated in both the kidneys and foot muscle of *C. chinensis*. Additionally, while most genes in the gills exhibited a trend towards increased expression under similar conditions, exceptions were noted for CchHSP20-02, CchHSP40-03, and CchHSP70-12.

Under low-temperature stress at 0 °C, the expression of CchHSP70-09 and CchHSP90-02 are elevated in the foot muscle. Notably, the expression of CchHSP10-01, CchHSP40-03, and CchHSP90-02 is significantly upregulated in the gills. Furthermore, an increase in the expression of both CchHSP40-03 and CchHSP90-02 is observed in the kidneys. The correlation coefficient for the expression levels of these CchHSPs across different tissues compared to the control group indicates that their expression patterns are tissue-specific and markedly influenced by temperature stress (Fig. 6).

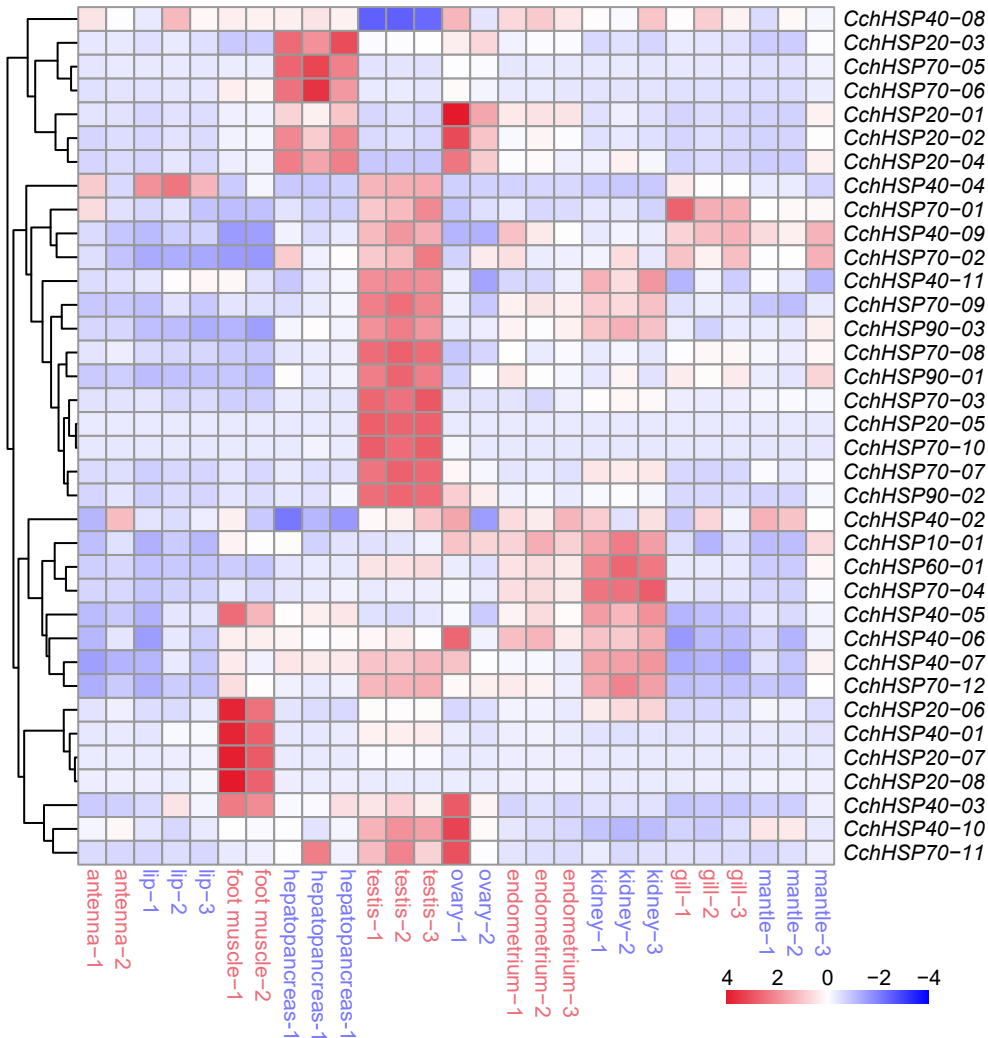


Fig. 5 The expression levels of CchHSPs in antennae, lip, foot muscle, testis, ovary, hepatopancreas, kidney, gill, endometrium, and mantle.

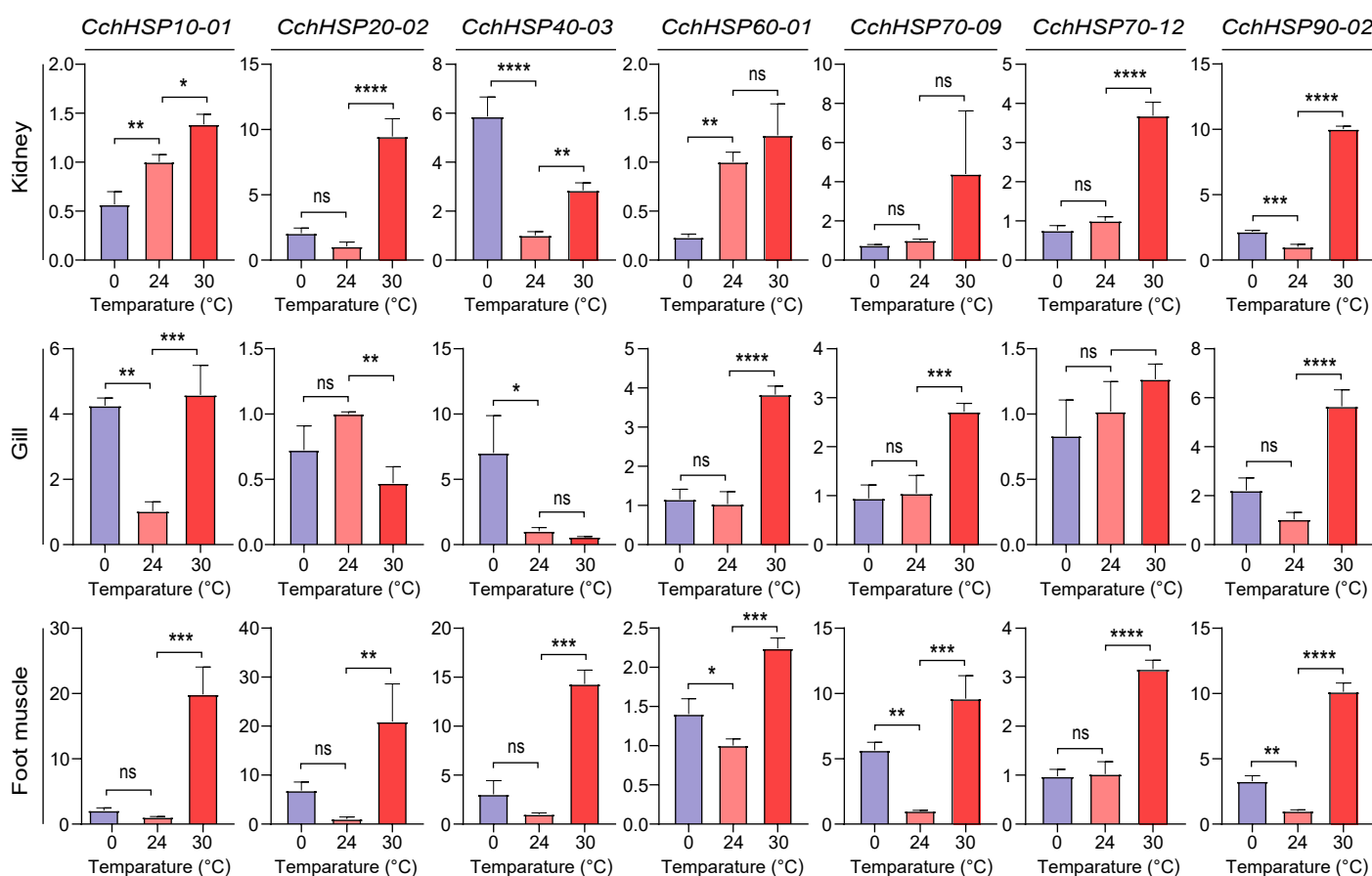


Fig. 6 Relative expression levels of CchHSPs in kidney, gill, and foot muscles under temperature stress. The horizontal axis is the temperature of temperature stress and the vertical axis is the relative expression level of genes.

Discussion

In this study, we utilized Hidden Markov Model (HMM) and homologous blast methods to identify the HSP gene family in *C. chinensis*. According to the physicochemical properties, the pI of CchHSPs ranges from 4.91 to 10.04, with a high proportion (77.78%) being acidic proteins which resembled the findings in *P. canaliculata*^[13], suggesting that CchHSPs primarily function under acidic conditions. Almost all CchHSPs are hydrophilic, and hydrophilic interactions play an important role in protein-protein association, assembly, the process of protein folding, and molecular recognition^[40,41]. Subcellular localization analysis shows that most CchHSPs are located in the cytoplasm, which is crowded with macromolecules. These proteins primarily perform functions such as protein folding and cell signaling in this cellular compartment^[42]. In addition, four sets of tandem duplicated genes were identified in this study on chromosomes 1, 2, 4, and 7. Tandem duplication is crucial for the expansion and evolution of gene families in organisms, as well as the generation of new functions^[43,44].

Gene structure analysis reveals that each family contains specific motifs and different gene domains, reflecting the functional differences among the subfamilies. There are significant variations in the size, number, and positions of introns and exons among CchHSPs. Notably, some genes lack introns, which resembled the situation in *P. canaliculata*^[13]. Some sister branches shared motifs, indicating that genes in the same subfamily have similar gene structures and functions. Significant motif differences among different subfamilies indicate potential functional differences among subfamilies. Most members within the same clade contain identical domains, suggesting they may perform similar functions. However, different domains

can exist within the same family. For example, the domains of *CchHSP90s* vary, likely due to the development of new functions in family members during evolution.

The secondary structure of CchHSPs mainly comprises alpha helices, extended strands, and random coils. HSPs regulate the folding, localization, accumulation, and degradation of protein molecules^[11]. A previous study reported that the alpha-helix structure of HSPs aids in faster protein folding^[45], while the extended strand structure forms intermolecular hydrogen bonds which are essential for chaperone function and establishes hydrophobic contacts with small HSP proteins, maintaining protein oligomerization and stability, thus fulfilling the protein chaperone function of HSPs^[7,46,47]. CchHSP60s, CchHSP70s, and CchHSP90s have a high proportion of alpha helices, which may facilitate rapid protein folding. CchHSP40s can collaborate with CchHSP70s to perform chaperone functions. This collaboration is facilitated by the J domain of the HSP40 subfamily protein, which is composed of alpha-helices that interact with HSP70 proteins to form a binary complex^[48]. According to the prediction of three-dimensional structure, it is speculated that genes with similar structures in sister branches of the same subfamily may have similar functions.

The phylogenetic tree of CchHSPs within the species in this study is divided into three branches: one branch consists of members of the CchHSP40 subfamily; one branch consists of members of the CchHSP70 subfamily; and one branch consists of members of other subfamilies. In the interspecific phylogenetic tree, members of various families from seven species cross-clustered together, suggesting that HSP gene subfamilies were formed before the divergence of these species.

Most CchHSPs exhibit tissue-specific expression. Previous studies have shown that *HSP10* is involved in the regulation of apoptosis in ovarian granulosa cells^[49], and *CchHSP10* may be involved in the regulation of follicular and oocyte development and maturation in *C. chinensis*. *CchHSP20-06*, *CchHSP20-07*, and *CchHSP20-08* are highly expressed in the foot muscles. *HSP20*, a chaperone protein abundantly expressed in smooth muscle, is a crucial regulator of muscle contraction, cell migration, and cell survival^[50]. This high expression in the foot muscles indicates that CchHSP20s may have a potential regulatory role in smooth muscle contraction in *C. chinensis*. Additionally, some CchHSP20s are highly expressed in the hepatopancreas. In *Procambarus clarkii*, immune elicitors significantly enhance *HSP20* expression in the hepatopancreas^[51], suggesting that CchHSP20s may participate in immune activities in this organ. CchHSP60s are predominantly expressed in the kidney, indicating a potential role in the complex communication network between the immune system and the body^[52]. *HSP60* acts as a ligand that activates B cells and regulates effector T cell activity through innate TLR2 signaling^[53]. The *HSP60* epitope is also recognized by T cells in both health and autoimmune diseases^[54]. *HSP70* and *HSP90* are primarily involved in the metabolism of non-reproductive organ epithelium, spermatogenic cells, and testicular mesenchymal cells^[55]. Some CchHSP70s and CchHSP90s are highly expressed in the testis, implying that these family members may play critical regulatory roles in testis development and spermatogenesis in *C. chinensis*. A previous study has shown that *HSP90* is intensely expressed in prespermatogonia and spermatogonia in rabbit testes^[56].

CchHSP70-9, CchHSP70-12, and CchHSP90-2 are key nodes in the PPI network, and they all interact with NEDD8, A0A2T7PA24, and A0A2T7NZM9 proteins. Previous studies have revealed that NEDD8 is a ubiquitin-like protein essential for protein degradation and regulation within cells^[57]. It is speculated that these interactions may regulate cell proliferation and apoptosis through the *NEDD8* gene. The *Elongin-C*, primarily involved in the metabolic processes of various substances, can act as the ubiquitin ligase E3 necessary for ubiquitin-mediated protein degradation^[58,59]. It shows strong interactions with CchHSP70-9, CchHSP70-12, CchHSP90-2, and NEDD8, suggesting a joint involvement in the ubiquitin-mediated protein degradation process.

The findings also demonstrated that there is also a strong interaction between A0A2T7PA24, A0A2T7NZM9, and the three key nodes. Both A0A2T7PA24 and A0A2T7NZM9 can bind to FK506 and are associated with prostaglandin-E synthase activity. Studies indicate that FK506 is involved in regulating the post-traumatic inflammatory process and has a neuroprotective effect on various cell populations in the central nervous system^[60]. A0A2T7NZM9 contains the STI1 domain^[61,62], which is present in many co-chaperone proteins and referred to as the heat shock chaperone protein binding domain. A0A2T7NZM9 received stimulation from cytokines and chemicals, so it is speculated that it is a stress-induced gene. It is hypothesized that A0A2T7NZM9 receives stimulation signals, activates the synthesis of HSP, and assists in the correct folding, assembly, and refolding of proteins along with A0A2T7PA24 and HSPs, which further binds to FK506 to reduce nerve damage and cell damage^[60].

Numerous studies have demonstrated that HSPs play a crucial role in response to both high- and low-temperature stress. For instance, in *Nacella concinna*, the expression levels of *HSP70* were elevated under heat stress and significantly reduced under cold stress^[63]. Similarly, in this study, *HSP70* showed increased expression under heat stress, with upregulation observed in the foot under

cold stress, while other tissues exhibited minimal changes. In *Laterula elliptica*, the expression level of *HSP70* in gills significantly increases under heat stress^[64]. For *Pinctada martensii*, the expression level of *HSP40* in the gills initially rise significantly under heat stress and then returns to baseline levels after 48 h^[65]. In this study, *CchHSP40-03* was significantly upregulated in the kidney and foot muscle after three days of heat stress, while the expression level in gills remained similar to the normal level, likely returning to baseline after the stress period which is similar to what happened in *P. martensii*. The expression of *CchHSP90-02* was up-regulated under cold stress and heat stress, and a similar situation also appeared in the muscle and skin of *Andrias davidianus*, indicating that *HSP90* plays an important role in coping with temperature stress^[66]. The expression levels of *HSP70* and *HSP90* in land snail species also increased continuously during the first 15–20 d after exposure to 34 °C^[67]. It can be seen that the HSP gene family plays an important role in the adaptability to temperature. The expression of CchHSPs is more sensitive to heat stress than cold stress, particularly in the foot muscle. Changes in the expression levels of *CchHSP40-3* in kidney and gill under cold stress were significant and even greater than the effects produced by heat stress. *HSP40* may play a key role in the adaptation of *C. chinensis* to cold environments.

Conclusions

In this study, we identified the HSP gene family associated with stress responses in *C. chinensis* at the whole-genome level. A total of 36 genes were identified, encompassing the *HSP10*, *HSP20*, *HSP40*, *HSP60*, *HSP70*, and *HSP90* subfamilies distributed across nine chromosomes, and some subfamilies exhibited gene duplication events.

Structural analysis indicated that each subfamily possesses specific sequence patterns and distinct structural domains, reflecting functional differences among them. Significant variations were observed in terms of size, number, and location of introns and exons within CchHSPs. The secondary structure of CchHSPs predominantly consisted of alpha helices, extended chains, and random coils.

Protein interaction analysis demonstrated that genes such as *CchHSP90-02*, *CchHSP70-12*, and *CchHSP70-09* occupied central positions within interaction networks, suggesting their core roles in cellular processes. It is worth noting that the expression levels of HSP genes in *C. chinensis* are significantly different in different tissues, indicating that these genes have different functional roles. The qPCR experiments assessing the expression profiles of the HSP gene family under cold and heat stress confirmed that *CchHSP70-09*, *CchHSP70-12*, and *CchHSP90-02* were highly expressed during these stresses, underscoring their important roles in stress response mechanisms.

This study provides a foundational data set and theoretical support for further investigations into the regulation of HSPs in relation to environmental adaptability, particularly temperature. Through these studies, we aim to offer more comprehensive theoretical insights into the molecular adaptation mechanisms and environmental resilience of *C. chinensis*.

Author contributions

The authors confirm contribution to the paper as follows: study conception and design: Wu X, Wang G, Chen H; data collection: Sun Q, Wei Z, Xuan F, Zhao S; analysis and interpretation of results: Yang W, Chen S, Jin W, Ji Q; draft manuscript preparation: Wu X, Wang G, Yang W, Sun Y; project organization and supervision: Tang B, Zhang D. All

authors reviewed the results and approved the final version of the manuscript.

Data availability

The transcriptome datasets generated and analyzed during the current study are available in the NCBI database: PRJNA1134349. The genomes of *B. aeruginosa* have been deposited in the Genome Warehouse at the NGDC, BIG, CAS / CNCB (BioProject: PRJCA032440).

Acknowledgments

This research was supported by the National Natural Science Foundation of China (32070526 and 32270487), the Key Research and Development Programme of Jiangsu Province (BE2020673), and the Major Project of Jiangsu Higher Education Institutions for Basic Science (Natural Science) Research (24KJA240003).

Conflict of interest

The authors declare that they have no conflict of interest.

Supplementary information accompanies this paper at (<https://www.maxapress.com/article/doi/10.48130/gcomm-0025-0009>)

Dates

Received 23 December 2024; Revised 3 April 2025; Accepted 11 April 2025; Published online 9 May 2025

References

- Jacob P, Hirt H, Bendahmane A. 2017. The heat-shock protein/chaperone network and multiple stress resistance. *Plant Biotechnology Journal* 15:405–14
- Saibil H. 2013. Chaperone machines for protein folding, unfolding and disaggregation. *Nature Reviews. Molecular Cell Biology* 14:630–42
- Hu C, Yang J, Qi Z, Wu H, Wang B, et al. 2022. Heat shock proteins: Biological functions, pathological roles, and therapeutic opportunities. *MedComm* 3:e161
- Kregel KC. 2002. Heat shock proteins: modifying factors in physiological stress responses and acquired thermotolerance. *Journal of Applied Physiology (Bethesda, Md.: 1985)* 92: 2177–86
- Beckmann RP, Lovett M, Welch WJ. 1992. Examining the function and regulation of hsp 70 in cells subjected to metabolic stress. *Journal of Cell Biology* 117:1137–50
- Srivastava P. 2002. Roles of heat-shock proteins in innate and adaptive immunity. *Nature Reviews Immunology* 2:185–94
- Haslbeck M, Vierling E. 2015. A first line of stress defense: small heat shock proteins and their function in protein homeostasis. *Journal of Molecular Biology* 427:1537–48
- Multhoff G, Botzler C. 1998. Heat-shock proteins and the immune response. *Annals of the New York Academy of Sciences* 851:86–93
- Takayama S, Reed JC, Homma S. 2003. Heat-shock proteins as regulators of apoptosis. *Oncogene* 22:9041–47
- Van Eden W, Wick G, Albani S, Cohen I. 2007. Stress, heat shock proteins, and autoimmunity: how immune responses to heat shock proteins are to be used for the control of chronic inflammatory diseases. *Annals of the New York Academy of Sciences* 1113:217–37
- Feder ME, Hofmann GE. 1999. Heat-shock proteins, molecular chaperones, and the stress response: evolutionary and ecological physiology. *Annual Review of Physiology* 61:243–82
- Zolkiewski M, Zhang T, Nagy M. 2012. Aggregate reactivation mediated by the Hsp100 chaperones. *Archives of Biochemistry and Biophysics* 520:1–6
- Gao Y, Li JN, Pu JJ, Tao KX, Zhao XX, et al. 2022. Genome-wide identification and characterization of the HSP gene superfamily in apple snails (Gastropoda: Ampullariidae) and expression analysis under temperature stress. *International Journal of Biological Macromolecules* 222:2545–55
- Yang C, Wang L, Liu C, Zhou Z, Zhao X, et al. 2015. The polymorphisms in the promoter of HSP90 gene and their association with heat tolerance of bay scallop. *Cell Stress & Chaperones* 20:297–308
- Bao Y, Wang Q, Liu H, Lin Z. 2011. A small HSP gene of bloody clam (*Tegillarca granosa*) involved in the immune response against *Vibrio parahaemolyticus* and lipopolysaccharide. *Fish & Shellfish Immunology* 30:729–33
- García de la Serrana D, Pérez M, Nande M, Hernández-Urcera J, Pérez E, et al. 2020. Regulation of growth-related genes by nutrition in paralarvae of the common octopus (*Octopus vulgaris*). *Gene* 747:144670
- Makhnevych T, Houry WA. 2012. The role of Hsp90 in protein complex assembly. *Biochimica et Biophysica Acta (BBA) - Molecular Cell Research* 1823:674–82
- Pratt WB. 1998. The hsp90-based chaperone system: involvement in signal transduction from a variety of hormone and growth factor receptors. *Proceedings of the Society for Experimental Biology and Medicine* 217:420–34
- Chen L, Yu F, Shi H, Wang Q, Xue Y, et al. 2022. Effect of salinity stress on respiratory metabolism, glycolysis, lipolysis, and apoptosis in Pacific oyster (*Crassostrea gigas*) during depuration stage. *Journal of the Science of Food and Agriculture* 102:2003–11
- Giffard RG, Yenari MA. 2004. Many mechanisms for hsp70 protection from cerebral ischemia. *Journal of Neurosurgical Anesthesiology* 16:53–61
- Li C, Li L, Liu F, Ning X, Chen A, et al. 2011. Alternation of *Venerupis philippinarum* Hsp40 gene expression in response to pathogen challenge and heavy metal exposure. *Fish & Shellfish Immunology* 30:447–50
- Guan H, Hu D, Zhao Z, Cai W, Zhou Q, et al. 2015. Role of Hsp-70 responses in cold acclimation of HUVEC-12 cells. *International Journal of Clinical and Experimental Medicine* 8:1880–87
- Zhang HP, Liu W, An JQ, Yang P, Guo LH, et al. 2021. Transcriptome analyses and weighted gene coexpression network analysis reveal key pathways and genes involved in the rapid cold resistance of the Chinese white wax scale insect. *Archives of Insect Biochemistry and Physiology* 107:e21781
- Junprung W, Norouzitallab P, De Vos S, Tassanakajon A, Nguyen Viet D, et al. 2019. Sequence and expression analysis of HSP70 family genes in *Artemia franciscana*. *Scientific Reports* 9:8391
- Lu HF, Du LN, Li ZQ, Chen XY, Yang JX. 2014. Morphological analysis of the Chinese *Cipangopaludina* species (Gastropoda; Caenogastropoda: Viviparidae). *Zoological Research* 35:510–27
- Tanaka M, Asahina H, Yamada N, Osumi M, Wada A, et al. 1987. Pattern and time course of cleavages in early development of the ovoviparous pond snail, *Sinotaia quadrata* *historica*. *Development, Growth & Differentiation* 29:469–78
- Szybiak K, Gabala E, Adamski Z. 2022. Different dynamics of reproductive cell development in *Oviparous Clausilia bidentata* and *Ovoviparous Ruthenica filograna* snails. *Zoological Studies* 61:e14
- Fang L, Wang S, Sun X, Wang K. 2024. Bioaccumulation and biochemical impact of polyethylene terephthalate microplastics in *Cipangopaludina chinensis*: Tissue-specific analysis and homeostasis disruption. *Aquatic Toxicology* 277:107144
- Chapman EEV, Moore C, Campbell LM. 2020. Evaluation of a nanoscale zero-valent iron amendment as a potential tool to reduce mobility, toxicity, and bioaccumulation of arsenic and mercury from wetland sediments. *Environmental Science and Pollution Research* 27:18757–72
- Altschul SF, Gish W, Miller W, Myers EW, Lipman DJ. 1990. Basic local alignment search tool. *Journal of Molecular Biology* 215:403–10
- Potter SC, Luciani A, Eddy SR, Park Y, Lopez R, et al. 2018. HMMER web server: 2018 update. *Nucleic Acids Research* 46:W200–W204
- Chen C, Chen H, Zhang Y, Thomas HR, Frank MH, et al. 2020. TBtools: An Integrative Toolkit Developed for Interactive Analyses of Big Biological Data. *Molecular Plant* 13:1194–202
- Bailey TL, Boden M, Buske FA, Frith M, Grant CE, et al. 2009. MEME SUITE: tools for motif discovery and searching. *Nucleic Acids Research* 37:W202–W208

34. Tamura K, Stecher G, Kumar S. 2021. MEGA11: molecular evolutionary genetics analysis version 11. *Molecular Biology and Evolution* 38:3022–27
35. Xie J, Chen Y, Cai G, Cai R, Hu Z, Wang H. 2023. Tree Visualization By One Table (tvBOT): a web application for visualizing, modifying and annotating phylogenetic trees. *Nucleic Acids Research* 51:W587–W592
36. Bolger AM, Lohse M, Usadel B. 2014. Trimmomatic: a flexible trimmer for Illumina sequence data. *Bioinformatics* 30:2114–20
37. Kim D, Paggi JM, Park C, Bennett C, Salzberg SL. 2019. Graph-based genome alignment and genotyping with HISAT2 and HISAT-genotype. *Nature Biotechnology* 37:907–15
38. Liao Y, Smyth GK, Shi W. 2014. featureCounts: an efficient general purpose program for assigning sequence reads to genomic features. *Bioinformatics* 30:923–30
39. Zhai Z, Chen X, Wang J. 2008. Primer Design with Primer Premier 5.0. *Northwest Medical Education* 16(4):695–98
40. Ben-Naim A. 2011. The rise and fall of the hydrophobic effect in protein folding and protein-protein association, and molecular recognition. *Open Journal of Biophysics* 1:1–7
41. Durell SR, Ben-Naim A. 2017. Hydrophobic-hydrophilic forces in protein folding. *Biopolymers* 107:e23020
42. Luby-Phelps K. 2013. The physical chemistry of cytoplasm and its influence on cell function: an update. *Molecular Biology of the Cell* 24:2593–96
43. Liu M, Sun W, Ma Z, Huang L, Wu Q, et al. 2019. Genome-wide identification of the SPL gene family in Tartary Buckwheat (*Fagopyrum tataricum*) and expression analysis during fruit development stages. *BMC Plant Biology* 19:299
44. Mehan MR, Freimer NB, Ophoff RA. 2004. A genome-wide survey of segmental duplications that mediate common human genetic variation of chromosomal architecture. *Human Genomics* 1:335–44
45. Motojima F. 2015. How do chaperonins fold protein? *Biophysics* 11:93–102
46. Bondino HG, Valle EM, Ten Have A. 2012. Evolution and functional diversification of the small heat shock protein/ α -crystallin family in higher plants. *Planta* 235:1299–313
47. Waters ER. 2013. The evolution, function, structure, and expression of the plant sHSPs. *Journal of Experimental Botany* 64:391–403
48. Knox C, Luke GA, Blatch GL, Pesce ER. 2011. Heat shock protein 40 (Hsp40) plays a key role in the virus life cycle. *Virus Research* 160:15–24
49. Ling J, Zhao K, Cui YG, Li Y, Wang X, et al. 2011. Heat shock protein 10 regulated apoptosis of mouse ovarian granulosa cells. *Gynecological Endocrinology* 27:63–71
50. Salinthon S, Tyagi M, Gerthoffer WT. 2008. Small heat shock proteins in smooth muscle. *Pharmacology & Therapeutics* 119:44–54
51. Li CS, Kausar S, Gul I, Yao XX, Li MY, et al. 2020. Heat shock protein 20 from *Procambarus clarkii* is involved in the innate immune responses against microbial infection. *Developmental and Comparative Immunology* 106:103638
52. Carmicle S, Steede NK, Landry SJ. 2007. Antigen three-dimensional structure guides the processing and presentation of helper T-cell epitopes. *Molecular Immunology* 44:1159–68
53. Gao XJ, Tang B, Liang HH, Yi L, Wei ZG. 2019. Selenium deficiency induced an inflammatory response by the HSP60 - TLR2-MAPKs signalling pathway in the liver of carp. *Fish & Shellfish Immunology* 87:688–94
54. Quintana FJ, Cohen IR. 2011. The HSP60 immune system network. *Trends in Immunology* 32:89–95
55. Cui Y, Liu P, Yu S, He J, Afedo SY, et al. 2022. Expression analysis of molecular chaperones Hsp70 and Hsp90 on development and metabolism of different organs and testis in cattle (cattle-yak and yak). *Metabolites* 12:1114
56. Wu Y, Pei Y, Qin Y. 2011. Developmental expression of heat shock proteins 60, 70, 90, and A2 in rabbit testis. *Cell and Tissue Research* 344:355–63
57. Kamitani T, Kito K, Nguyen HP, Yeh ET. 1997. Characterization of NEDD8, a developmentally down-regulated ubiquitin-like protein. *The Journal of Biological Chemistry* 272:28557–62
58. Hori T, Osaka F, Chiba T, Miyamoto C, Okabayashi K, et al. 1999. Covalent modification of all members of human cullin family proteins by NEDD8. *Oncogene* 18:6829–34
59. Schwechheimer C. 2018. NEDD8-its role in the regulation of Cullin-RING ligases. *Current Opinion in Plant Biology* 45:112–19
60. Saganová K, Gálik J, Blaško J, Korimová A, Račková E, et al. 2012. Immunosuppressant FK506: focusing on neuroprotective effects following brain and spinal cord injury. *Life Sciences* 91:77–82
61. Fry MY, Saladi SM, Clemons WM Jr. 2021. The STI1-domain is a flexible alpha-helical fold with a hydrophobic groove. *Protein Science: A Publication of the Protein Society* 30:882–98
62. Letunic I, Bork P. 2018. 20 years of the SMART protein domain annotation resource. *Nucleic Acids Research* 46:D493–D496
63. Clark MS, Peck LS. 2009. Triggers of the HSP70 stress response: environmental responses and laboratory manipulation in an Antarctic marine invertebrate (*Nacella concinna*). *Cell Stress & Chaperones* 14:649–60
64. Park H, Ahn IY, Lee HE. 2007. Expression of heat shock protein 70 in the thermally stressed antarctic clam *Laternula elliptica*. *Cell Stress & Chaperones* 12:275–82
65. Li J, Zhang Y, Liu Y, Zhang Y, Xiao S, et al. 2016. Co-expression of heat shock protein (HSP) 40 and HSP70 in *Pinctada martensii* response to thermal, low salinity and bacterial challenges. *Fish & Shellfish Immunology* 48:239–43
66. Li G, Xu K, Yang W, Luo J, HUANG, DU X. 2019. cDNA cloning of heat shock protein Hsp90 gene in *Andrias davidianus* and its expression exposed to extreme temperature stress. *Jiangsu Agricultural Sciences* 47(24):34–39
67. Staikou A, Sagonas K, Spanoudi O, Savvidou K, Nazli Z, et al. 2024. Activities of antioxidant enzymes and Hsp levels in response to elevated temperature in land snail species with varied latitudinal distribution. *Comparative Biochemistry and Physiology Part B: Biochemistry and Molecular Biology* 269:110908



Copyright: © 2025 by the author(s). Published by Maximum Academic Press, Fayetteville, GA. This article is an open access article distributed under Creative Commons Attribution License (CC BY 4.0), visit <https://creativecommons.org/licenses/by/4.0/>.